



PERGAMON

Deep-Sea Research II 49 (2002) 921–933

DEEP-SEA RESEARCH
PART II

www.elsevier.com/locate/dsr2

Sediment accumulation rates and carbon fluxes to bottom sediments at the Western Bransfield Strait (Antarctica)

Pere Masqué^{a,c,*}, Enrique Isla^b, Joan A. Sanchez-Cabeza^a, Albert Palanques^b,
Joan M. Bruach^a, Pere Puig^{b,d}, Jorge Guillén^b

^a *Departament de Física, Universitat Autònoma de Barcelona, E-08193 Bellaterra, Spain*

^b *Institut de Ciències del Mar (CSIC, CMIMA), Passeig Marítim de la Barceloneia 37-49, E-08003 Barcelona, Spain*

^c *Marine Sciences Research Center, State University of New York, Stony Brook, NY 11794-5000, USA*

^d *School of Oceanography, University of Washington, Box: 357940, Seattle, WA 98195, USA*

Received 27 January 2000; received in revised form 22 June 2000; accepted 8 June 2001

Abstract

Mean sediment and carbon accumulation rates in the western Bransfield Strait, during the last ca. 100 years, were determined at three sites by using ^{210}Pb as a radiotracer of sedimentation processes. ^{210}Pb profiles showed moderate mixing in the upper 8.5–12 cm, which was attributed to bioturbation. Sediment accumulation rates calculated assuming no mixing below the surface mixed layer (SML) were found to be relatively high (between 0.03 and $0.09 \text{ g cm}^{-2} \text{ yr}^{-1}$), in good agreement with previously reported data based on both ^{210}Pb and ^{14}C dating in surrounding areas. These results, together with the calculated excess ^{210}Pb fluxes to the bottom sediments and the ^{210}Pb and ^{210}Po distributions in the water column, indicated the presence of a large net advective flux of material in the area, highlighting the importance of glacial related sedimentation processes in this semi-enclosed sea. Carbon in bottom sediments was mainly organic, and its content was moderately low (0.65–1.25%), being slightly higher within the SML, reflecting the presence of inhabiting organisms. However, organic carbon (OC) accumulation fluxes (3.1 – $6.7 \text{ g C m}^{-2} \text{ yr}^{-1}$) were considerable, due to the high sediment accumulation rates. ^{210}Pb dated profiles allowed us to estimate the amount of carbon exported from the water column and buried in the bottom sediment, which represents about 3–7% of the mean annual primary production in the euphotic layer of the Bransfield Strait. The burial efficiency of OC in the sediment was estimated to be approximately 60–80%. © 2001 Published by Elsevier Science Ltd.

1. Introduction

Studies from ice-core measurements have indicated that the atmospheric partial pressure of

CO_2 , the most important greenhouse gas in the atmosphere after water vapour, has increased by about 32% from the beginning of the industrial revolution (Neftel et al., 1985). From emission estimates (Marland et al., 1999) and tropospheric $p\text{CO}_2$ measurements (Keeling and Whorf, 1999) it can be deduced that the oceans and the terrestrial biosphere take up about 50% of anthropogenic emissions. The ocean alone presumably takes up about 35% of the anthropogenic emissions. There-

*Corresponding author. Marine Sciences Research Center, State University of New York, Stony Brook, NY 11794-5000, USA. Fax: +34-3-5812155.

E-mail address: pmasque@uab.es (P. Masqué).

fore, the understanding of the biogeochemical cycling of carbon in the oceans is important in the context of the removal of man-made carbon dioxide from the atmosphere. Heinze et al. (1999) recently stated that advances in marine carbon cycle research are urgently needed for both the inorganic as well as the biological CO_2 pumps to assess the role that the oceans play in the CO_2 cycle. In particular, it is essential to improve the quantitative interpretation of the marine sediment signal of the carbon cycle and climate changes; that is, the extent to which bottom sediments act as a sink for atmospheric CO_2 and, hence, whether burial of organic matter removes a significant fraction of carbon dioxide from the ocean-atmosphere system (Walsh et al., 1985).

Sarmiento and Toggweiler (1984) suggested that both biogeochemical cycles and water circulation in the Southern Ocean play an important role in controlling atmospheric carbon dioxide levels,

which in turn affect global climate. Field measurements and numerical models suggest that the Southern Ocean is currently a net sink for CO_2 , with the region south of 50°S accounting for ca. 20% of the global marine sink. The Antarctic continental margin is considered to be one of the most sensitive areas to climatic change, and therefore bottom sediments are considered to be important archives for the investigation of past climatic transitions. The Bransfield Strait, characterised by its high productivity (Huntley et al., 1991; Álvarez et al., 2002), therefore has a potential as a sink for atmospheric CO_2 (Anadón and Estrada, 2002).

The Bransfield Strait is a semi-enclosed Antarctic sea comprising an area of about $50,000 \text{ km}^2$ between the South Shetlands archipelago and the Antarctic Peninsula (Fig. 1). Gràcia et al. (1997) described the Bransfield Strait as a narrow, volcanic and seismically active extensional basin.

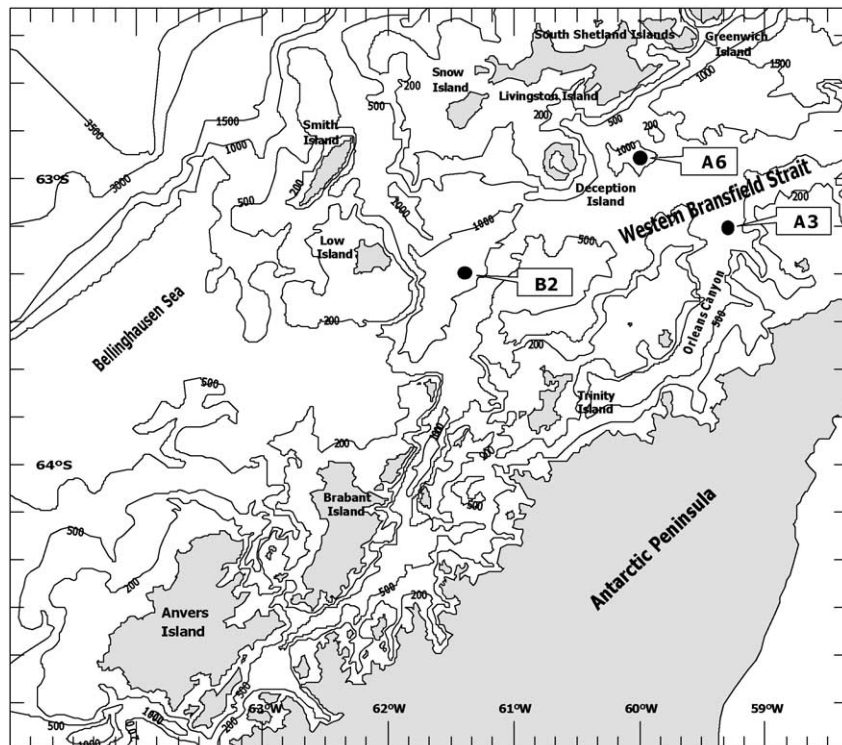


Fig. 1. Bottom sediment sampling stations in the western Bransfield Strait. Water samples at different depths were also collected at station A-6.

It can be divided into three sub-basins separated from each other by sills shallower than 1000 m. Maximum depths in the Bransfield Strait are deeper than 2500 m in the eastern basin, 1950 m in the central basin and 1200 m in the western basin (Gràcia et al., 1997; Canals et al., 2000). The western Bransfield Strait is connected to the neighbouring Bellingshausen Sea to the west through passages between the westernmost South Shetland Islands and the Gerlache Strait, and to the Drake Passage to the north via the Boyd Strait. Connections also exist between interinsular passages, and through the northern mouth of the eastern Bransfield Basin.

The western basin has narrow (20–50 km wide) continental shelves and steep slopes, especially on the northern perimeter of the Antarctic Peninsula margin (Canals et al., 2000). The continental shelf is mainly covered by coarse sediments, whereas the deep basin receives fine sediments probably winnowed by bottom currents and transported laterally (Anderson et al., 1991; Palanques et al., 2002). Near-bottom particle fluxes are about three orders of magnitude higher than those of the middle depth, supplying most of the organic components by advective transport (Palanques et al., 2002). From the hydrographic point of view, the Bransfield Strait is best defined as a transition zone between the Bellingshausen Sea and the Weddell Sea.

Radionuclides can be used to obtain sediment geochronologies and accumulation rates at different time scales. Therefore, they can be used to provide the temporal frame for the assessment of the evolution of parameters such as organic carbon (OC), which is a requirement to set up the carbon balance. Naturally occurring particle-reactive radionuclides are useful for quantifying mixing and accumulation rates in marine sediments (Koide et al., 1972; Guinasso and Shink, 1975; Benninger et al., 1979; Cochran, 1985). ^{210}Pb , a member of the ^{238}U decay series with a half-life of 22.3 yr, enters the oceans mainly via the atmosphere and through in situ production from radioactive decay of dissolved ^{226}Ra . Inputs from rivers also can occur in coastal areas. The higher affinity of ^{210}Pb for fine-grained particles and organic matter compared to that of ^{226}Ra causes

an excess of ^{210}Pb with respect to ^{226}Ra in the settling particles that are subsequently deposited on the sea floor. Assuming a constant flux of ^{210}Pb to the sea bed, excess ^{210}Pb in the sediments can be used to estimate recent (ca. 100 yr) sediment accumulation rates and the degree of mixing produced by the action of living organisms inhabiting the sediments or by physical agents (Goldberg, 1963; Appleby and Oldfield, 1978, 1992; DeMaster and Cochran, 1982; Zuo et al., 1997; Sanchez-Cabeza et al., 1999).

In this work we selected three stations in the western Bransfield Basin to determine the recent (ca. 100 yr) sediment accumulation and mixing rates, and the OC fluxes to bottom sediments, burial rates and the fraction preserved with respect to production. In addition, the ^{210}Pb and ^{210}Po behaviour in the water column at one of these stations was investigated to obtain a simple model for balancing ^{210}Pb in the overlying water column.

2. Field and laboratory methods

2.1. Bottom sediments

Bottom sediments from the western Bransfield Strait were collected using a multiple corer (Bowers and Connelly) designed to recover up to eight replicates 10 cm in diameter. All studied samples presented a layer of clear sea water over the top of the sediment, thus indicating that very low, if any, disturbance of the samples was induced due to insertion of the tube. Cores were collected in January and February 1996 during the research expedition *FRUELA-96* on board the Spanish research vessel *BIO Hespérides*. Three cores (A-3, A-6 and B-2) were selected for ^{210}Pb analysis. Station A-3 was located at the mouth of the Orleans Canyon, while station A-6 was south of Livingston Island and east of Deception Island and B-2 in a basin east of Low Island (Fig. 1).

Sediment core lengths ranged from 34 to 40 cm. One core from each station was subsampled at 0.5–2-cm intervals from top to bottom and sections were stored and frozen in sealed plastic bags until analysis. The outer 2 mm were removed

from each section to discard the sediment possibly smeared downward during core insertion. For each section, wet and dry densities were determined before and after drying samples at 40°C. About half of the sample was homogenised for carbon, nitrogen and radionuclide analyses, which included ^{210}Pb and gamma-emitters. The remaining non-homogenised sediment was used to determine sand content.

2.2. Determination of sand content

The sand percentage was obtained by sieving through a 63- μm mesh sieve a pre-weighed sample previously treated with peroxide (20%). The material collected on the sieve was rinsed with distilled water and then placed in an oven at 90°C for 24 h before weighing.

2.3. Water column

At station A-6, 301 water samples were collected with 12-l Niskin bottles with an oceanographic rosette, from eight depths (10, 20, 150, 250, 500, 650, 950 and 1059 m) to determine ^{210}Pb and ^{210}Po concentrations. Samples were immediately filtered through Schleicher&Schuell membrane filters to separate dissolved (<0.2 μm) and particulate (>0.2 μm) fractions. From each sample, an aliquot of 3–5 l was filtered through a 0.2 μm pore pre-weighed Nuclepore polycarbonate filter to determine the concentration of suspended particulate matter (SPM). The fraction for the determination of the dissolved species was immediately acidified to pH = 1 using HCl. Known amounts of ^{209}Po (half-life = 102 yr) and stable Pb^{2+} were added as internal tracers, as well as Fe^{3+} as a carrier for co-precipitation of lead and polonium isotopes as hydroxides after addition of NaOH. Filters containing the retained particulate matter and precipitates were stored in sealed plastic bags and plastic containers, respectively, until analysis in the laboratory.

2.4. Radiometric analysis

^{210}Pb analyses of the sediment samples were performed following the methodology described

by Sanchez-Cabeza et al. (1998), by total digestion of 200–300 mg sample aliquots. ^{209}Po was added to each sample before digestion as internal tracer. After digestion, samples were made 1 N HCl, and ^{209}Po and ^{210}Po were deposited onto silver disks at 60–70°C for 8 h while stirring. Polonium isotopes were counted with α -spectrometers equipped with low-background SSB detectors (EG&G Ortec). Due to the elapsed time span between sediment sampling and analyses, ^{210}Pb was assumed to be in radioactive equilibrium with ^{210}Po (half-life = 138 d) in the sediment samples.

Some dried and homogenised samples from each core were counted by gamma spectrometry in calibrated geometries for $2\text{--}3 \times 10^5$ s using a high-purity intrinsic Ge detector, surrounded by a 12 cm lead shield, lined with 1 cm copper and 2 mm cadmium, and linked to an 8 K MCA. Spectra were analysed with a modified version of the SAMPO family of programs (Koskelo et al., 1981). ^{226}Ra activities were determined through ^{214}Pb (351.92 keV) and ^{214}Bi (609.4 keV) lines of gamma emissions, assuming secular equilibrium with ^{226}Ra . No ^{137}Cs was detected along the cores by gamma spectrometry, due to the combined effects of low concentrations and small amounts of sample available.

Filters containing SPM for ^{210}Pb and ^{210}Po analyses were digested using *aqua regia* after addition of ^{209}Po , while precipitates were centrifuged in order to reduce volumes. All samples were made 1 N with HCl, and the same procedure described for sediment samples was followed. As analyses were carried out within 3 months after sample collection, equilibrium between ^{210}Po and ^{210}Pb had not yet been reached. One year after the first analyses, samples were reanalysed for ^{210}Po , present by in situ disintegration of ^{210}Pb , thus permitting us to determine both ^{210}Pb and ^{210}Po activities at the sample collection date after appropriate decay corrections.

Chemical recoveries of all radiochemical separations ranged from 85% to 100%. For each batch of 10 samples, a reagent blank analysis also was carried out and subtracted for activity determination.

2.5. Carbon and nitrogen

Total carbon (TC%) and nitrogen (N%) were measured in duplicate using a Leco CN 2000 analyser. Two subsamples were used to determine the total carbon percentage (TC%). Two other subsamples were digested with HCl in a LECO CC 100 digester and the resultant CO₂ was analysed in the LECO CN 2000 analyser, which was used to calculate the calcium carbonate concentration (CaCO₃%). The difference between the two values was assumed to represent the percentage of organic carbon content (OC%).

3. Results and discussion

Cores A-3 and B-2 consisted of muds with very low sand contents (2.8 ± 0.2% and 1.8 ± 0.2%, respectively), whereas at station A-6 the sand content was higher (13.2 ± 0.4%). The major components of the mud fraction were lithogenic minerals coming from weathering of the volcanic terrain on the Antarctic Peninsula and islands of the Bransfield Strait. The mud also showed a relatively high content of biogenic components,

especially biogenic opal (Holler, 1989; Yoon et al., 1994; Banfield and Anderson, 1995).

3.1. Excess ²¹⁰Pb concentration profiles in bottom sediments

Supported ²¹⁰Pb in bottom sediments was calculated from the constant activity of the deepest samples in the cores and was subtracted from the ²¹⁰Pb total activities to obtain the excess ²¹⁰Pb. Good agreement was found between the supported ²¹⁰Pb mean activities derived from alpha measurements (63.3 ± 2.8, 46.2 ± 0.7 and 31.3 ± 1.1 Bq kg⁻¹ for cores A-3, A-6 and B-2, respectively) and ²²⁶Ra mean activities obtained by gamma counting at several depths, which ranged from 35.5 to 54.4 Bq kg⁻¹. All data are plotted versus accumulated mass (Fig. 2) to avoid the shape of the profile being affected by variation in porosity along the core.

Excess ²¹⁰Pb extended to different depths at the three sites (maximum of 36 cm for core B-2, 25 and 16 cm for cores A-3 and A-6, respectively), which is a preliminary indication of the different sediment accumulation rates at the three sites. In all

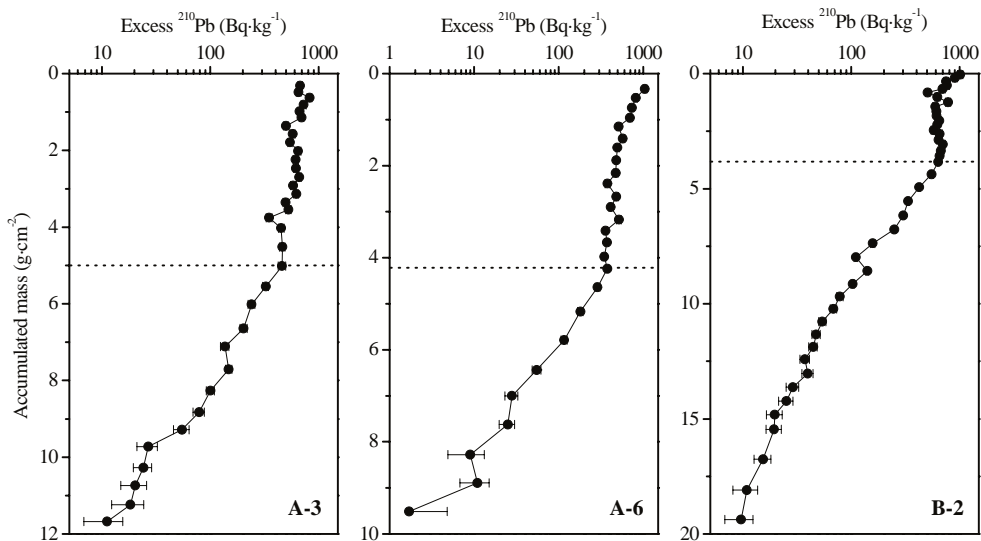


Fig. 2. Excess ²¹⁰Pb profiles versus mass accumulation in three cores from the western Bransfield Strait. Error bars denote the uncertainty in the activities determined from counting statistics (± 1σ). Dotted lines indicated the depth to which a surface mixed layer (SML) was estimated to be present.

Table 1

Sediment accumulation rates and main ^{210}Pb results for sediment cores A-3, A-6 and B-2 collected from the western Bransfield Strait

Core	Location		Depth (m)	Excess ^{210}Pb			Mixed layer		Mean sedimentation rate	
	Latitude S	Longitude W		Surface (Bq kg^{-1})	Inventory (kBq m^{-2})	Flux ($\text{Bq m}^{-2}\text{yr}^{-1}$)	Depth (SML) (cm)	D_B ($\text{cm}^2\text{yr}^{-1}$)	($\text{g cm}^{-2}\text{yr}^{-1}$)	(mm yr^{-1})
A-3	63° 10'	59° 20'	790	676±32	35.9±0.4	1097±13	12	12	0.060±0.003	1.17±0.05
A-6	62° 56'	60° 00'	1066	1046±54	26.3±0.3	803±11	8.5	2	0.0351±0.0014	0.57±0.02
B-2	63° 20'	61° 23'	1135	1010±59	42.3±0.3	1293±11	10	40	0.093±0.003	1.56±0.05

cores, a surface mixed layer (SML) was present in the upper 8.5–12 cm of the sediment (Table 1; Fig. 2). In fact, the SML presence led to an almost constant excess ^{210}Pb activity, especially in the case of core B-2, thus indicating the high degree of mixing. An exponential decrease of ^{210}Pb activity below the SML was observed in all cores, which was used to determine the mean sediment accumulation rates.

Surface excess ^{210}Pb concentrations in cores A-6 and B-2, which were collected from similar depths, were comparable (1046 ± 54 and 1010 ± 59 Bq kg^{-1} , respectively) but lower in core A-3 (676 ± 32 Bq kg^{-1}) (Table 1). Excess ^{210}Pb inventories, $A(0)$, ranging from 26.3 to 42.3 kBq m^{-2} , were calculated by summing the excess ^{210}Pb activity of each section. These results agree well with those given by Harden et al. (1992) for the Bransfield Strait, who reported a range of surface excess ^{210}Pb from 268 to 1610 Bq kg^{-1} and of excess ^{210}Pb inventories from 15 to 66 kBq m^{-2} . The annual excess ^{210}Pb fluxes to the sediment, q , were obtained by applying the equation proposed by Sanchez-Cabeza et al. (2000)

$$q = \frac{A(0)}{\Delta t}(1 - e^{-\lambda\Delta t}). \quad (1)$$

The use of this formula instead of the usual one ($q = \lambda A(0)$) allowed us to assume that the flux of ^{210}Pb to the sediments is constant during a period of time Δt (order of magnitude of years), instead of being continuously constant. In this work, Δt was taken as one year assuming that the *unsupported* ^{210}Pb flux to the sediment is time dependent, though the annual variations are possibly small (Turekian et al., 1977; Tsunogai et al., 1988;

Heussner et al., 1990; Thunell and Moore, 1994). From Eq. (1), the highest excess ^{210}Pb annual flux was obtained for core B-2 (1293 ± 11 $\text{Bq m}^{-2}\text{yr}^{-1}$), it being significantly lower for the other two stations (Table 1).

3.2. Sediment accumulation rates

Sediment reworking due to physical or biological agents may affect the excess ^{210}Pb distribution along the sediment. Therefore, basic hypotheses must take into account this factor so as not to overestimate sedimentation rates (Benninger et al., 1979; Nittrouer et al., 1984; Cochran, 1985). Goldberg and Koide (1962) pointed out that the main processes governing excess ^{210}Pb profiles in the seabed are sediment accumulation, radioactive decay and particle mixing. They proposed a one-dimensional advection–diffusion model to calculate the sedimentation rate (S , in cm yr^{-1}) and the mixing coefficient (D_B , in $\text{cm}^2\text{yr}^{-1}$) that describes the intensity of particle reworking

$$\frac{\partial A}{\partial t} = D_B \frac{\partial^2 A}{\partial x^2} - S \frac{\partial A}{\partial x} - \lambda A, \quad (2)$$

where A (Bq kg^{-1}) is the excess ^{210}Pb concentration at depth x (cm), and S and D_B are assumed to be constant.

Many researchers have used this procedure in continental-margin and deep-sea sediments (i.e. Guinasso and Shink, 1975; DeMaster and Cochran, 1982; Roberts et al., 1997). As D_B and S cannot be determined independently, a solution for D_B can be obtained if S is known or assumed to be negligible. When the latter is not the case or no evidence supporting this is available, S can be

determined in other ways, such as ^{14}C dating or ^{210}Pb from the non-mixed layer, where D_B is assumed negligible. In this respect, although comparison of ^{210}Pb sedimentation rates with those calculated from ^{14}C date may be useful, it must be done with caution because the two methodologies involve different time-scales.

Assuming steady state conditions and no mixing, Eq. (2) can be solved under the boundary conditions of $A = A_0$ ($x = 0$) and $A \rightarrow 0$ ($x \rightarrow \infty$), by means of the equation

$$A = A_0 e^{-(\lambda/S)x}. \quad (3)$$

This is usually done by least-squares fitting of the logarithm of excess ^{210}Pb versus depth for the strata below the SML. Then, the sedimentation rate calculated by using Eq. (3) or from ^{14}C data can be introduced as a constant in Eq. (4) to determine D_B , also using least-square fitting for the SML

$$A = A_0 e^{(S - \sqrt{S^2 + 4\lambda D_B})/2D_B x}. \quad (4)$$

In fact, as one cannot be sure that deep mixing is not present, Eq. (3) allows us to obtain an apparent sediment accumulation rate that may be an upper limit (Benninger et al., 1979; Nittrouer et al., 1984; Ledford-Hoffman et al. 1986). Some authors (e.g., Roberts et al., 1997) also simplify Eq. (4) by assuming that sediment accumulation is negligible in the mixed layer and the obtained mixing coefficient D_B is also an upper limit.

In this study, we consider the ^{210}Pb profiles as a two-layer system with an upper mixed layer extending to a distance L below the water-sediment interface (SML) and a second layer below L where no mixing takes place. Nelson (1988), DeMaster et al. (1991) and Harden et al. (1992) also used this procedure for determining accumulation rates and mixing coefficients in some cores from the Antarctic Peninsula area.

The highest sediment accumulation rate was obtained for core B-2 ($0.093 \pm 0.003 \text{ g cm}^{-2} \text{ yr}^{-1}$, or $1.56 \pm 0.05 \text{ mm yr}^{-1}$), being slightly higher than at station A-3 ($0.060 \pm 0.003 \text{ g cm}^{-2} \text{ yr}^{-1}$, or $1.17 \pm 0.05 \text{ mm yr}^{-1}$) and almost three times higher than that observed at station A-6 ($0.0351 \pm 0.0014 \text{ g cm}^{-2} \text{ yr}^{-1}$, or $0.57 \pm 0.02 \text{ mm yr}^{-1}$). There-

fore, sedimentation is relatively high at all three stations, with particular emphasis at B-2. The mixing coefficient was also higher at station B-2 ($40 \text{ cm}^2 \text{ yr}^{-1}$), which is fed by fines coming from the highly productive Gerlache Strait and adjacent fjords, than at stations A-3 and A-6 (12 and $2 \text{ cm}^2 \text{ yr}^{-1}$, respectively).

In general, ^{210}Pb -derived accumulation rates must be taken with prudence, and independent methods, such as ^{14}C dates or ^{137}Cs or $^{239,240}\text{Pu}$ chronologies, should be used to verify the results. This has been remarked on by various authors for southern high latitude environments (Ledford-Hoffman et al., 1986; DeMaster et al., 1991, 1996; Harden et al., 1992). ^{137}Cs , a consequence of the atmospheric detonation of nuclear weapons, has been in the seabed sediments since the early 1950s. Therefore, it can be used to quantify mixing in the surface sediments and how it affects the ^{210}Pb profiles. However, we were not able to detect ^{137}Cs by gamma spectrometry because levels are very low (Harden et al., 1992), although DeMaster et al. (1991) stated that in the Bransfield Strait the ^{137}Cs -penetration depth confirmed that deep mixing would be negligible in most cases.

^{14}C is commonly used to check the validity of the sediment accumulation rates inferred from ^{210}Pb profiles, as its longer half-life (5730 yr) allows it to be detected deeper in the sediment, presumably not affected by recent mixing processes (e.g. Nozaki et al., 1977). In a companion paper (Bárcena et al., 2002), ^{14}C -derived sediment accumulation rates have been calculated for stations A-3 (2.08 mm yr^{-1}) and A-6 (1.15 mm yr^{-1}). Taking into account the different time scales addressed by both dating techniques, these values agree reasonably well with those obtained using the ^{210}Pb method, particularly since differences between the two dating methods often can be as high as one order of magnitude. For instance, Harden et al. (1992) reported discrepancies between ^{210}Pb and ^{14}C sediment accumulation rates at two stations in Marguerite Bay (Pacific margin of the Antarctic Peninsula) and the Bransfield Strait as 2.5 and 0.4 mm yr^{-1} and 2.0 and 0.9 mm yr^{-1} , respectively. Moreover, the results for sedimentation rates reported by Demaster et al. (1991) and Harden et al. (1992) for

the Bransfield Strait ($1.2\text{--}2.3\text{ mm yr}^{-1}$) compare well with ours. Sedimentation rates obtained from ^{14}C in gravity cores at stations A-3 and A-6 were introduced in Eq. (4) and confirmed the mixing rates for the cores collected using the maxicorer system were not significantly different ($10\text{ cm}^2\text{ yr}^{-1}$ for A-3 and $12\text{ cm}^2\text{ yr}^{-1}$ for A-6) from those derived by using the ^{210}Pb sedimentation rates. For core B-2, as no ^{14}C derived accumulation rates were available, both the accumulation rate and the mixing coefficient derived from ^{210}Pb data were assumed to be reliable.

Palanques et al. (2002) has reported mass fluxes and ^{210}Pb data obtained from a sediment trap deployed 30 m above the sea floor at station A-6 for one year. The estimated mass flux was $0.13\text{ g cm}^{-2}\text{ yr}^{-1}$, the mean ^{210}Pb activity was $987 \pm 9\text{ Bq kg}^{-1}$, and the annual ^{210}Pb flux was $1310 \pm 12\text{ Bq m}^{-2}\text{ yr}^{-1}$. The mean ^{210}Pb activities in the material collected by the sediment trap and at the surface of core A-6 ($1046 \pm 54\text{ Bq kg}^{-1}$) were similar (ratio trap/core = 0.94), indicating that the material collected by the sediment trap is of the same nature as that which ultimately accumulates on the sea floor. It is worth mentioning that although ^{226}Ra contents in sediment trap material were not corrected, such corrections were not critical since concentrations usually found in sinking material (between $30\text{--}60\text{ Bq kg}^{-1}$) are low compared to excess ^{210}Pb .

In contrast, some discrepancies are observed when comparing both mass and ^{210}Pb fluxes, as annual trap values were, respectively, 3.8 and 1.6 times higher than those derived from ^{210}Pb dating

of bottom sediments. Direct comparison between sediment and trap data, however, must be done with caution, as time scales differ by a factor of about 100. However, the sediment trap fluxes do confirm that sediment accumulation in this area is high, of the order of that observed in bottom sediments, and sufficient to discard the hypothesis that mixing is the only process that accounts for the presence of excess ^{210}Pb downcore to 20–25 cm depth.

3.3. ^{210}Pb and ^{210}Po in the water column

^{210}Pb and ^{210}Po concentrations in the dissolved fraction were almost constant along the entire water column, with ^{210}Pb systematically in excess (ratio $^{210}\text{Po}/^{210}\text{Pb} = 0.48 \pm 0.02$) at all depths (Table 2). In the particulate fraction, ^{210}Pb concentration increased almost monotonically with depth, from $0.071 \pm 0.006\text{ Bq m}^{-3}$ (4% of the total ^{210}Pb) at the surface to $0.28 \pm 0.02\text{ Bq m}^{-3}$ (14% of the total ^{210}Pb) at 10 m above the sea floor. As ^{210}Pb is scavenged by sinking particles, this suggests that the residence time of particles is responsible for this enrichment. Particulate ^{210}Po , representing about 25% of the total ^{210}Po , showed a similar pattern with the exception of concentrations observed in surface waters (10 and 20 m), where maximum activities were found.

The $^{210}\text{Po}/^{210}\text{Pb}$ ratios in the particulate fraction at 10 and 20 m were 4.5 ± 0.5 and 5.3 ± 0.6 , respectively. It is usually accepted (Heyraud and Cherry, 1983) that the average $^{210}\text{Po}/^{210}\text{Pb}$ ratio is 0.5 in surface waters, 1 in sediments, 2 in

Table 2
 ^{210}Pb and ^{210}Po vertical profiles in the water column at station A-6

Depth (m)	^{210}Pb (Bq m^{-3})			^{210}Po (Bq m^{-3})			$^{210}\text{Po}/^{210}\text{Pb}$ ratio		
	Total	Particulate	Dissolved	Total	Particulate	Dissolved	Total	Particulate	Dissolved
10	1.72 ± 0.11	0.071 ± 0.006	1.65 ± 0.11	0.99 ± 0.08	0.32 ± 0.02	0.67 ± 0.07	0.57 ± 0.06	4.5 ± 0.5	0.40 ± 0.05
20	1.65 ± 0.11	0.066 ± 0.007	1.58 ± 0.11	1.28 ± 0.10	0.35 ± 0.02	0.92 ± 0.09	0.77 ± 0.08	5.3 ± 0.6	0.58 ± 0.07
150	2.14 ± 0.10	0.116 ± 0.008	2.03 ± 0.10	1.00 ± 0.09	0.16 ± 0.02	0.84 ± 0.09	0.46 ± 0.05	1.4 ± 0.2	0.41 ± 0.05
250	3.09 ± 0.14	0.146 ± 0.014	2.95 ± 0.14	0.60 ± 0.08	0.17 ± 0.02	0.43 ± 0.08	0.19 ± 0.03	1.2 ± 0.2	0.15 ± 0.03
500	2.17 ± 0.11	0.173 ± 0.014	1.99 ± 0.11	1.19 ± 0.10	0.23 ± 0.02	0.96 ± 0.10	0.55 ± 0.05	1.3 ± 0.2	0.48 ± 0.06
650	2.04 ± 0.10	0.21 ± 0.02	1.83 ± 0.09	1.18 ± 0.08	0.27 ± 0.02	0.92 ± 0.08	0.58 ± 0.05	1.3 ± 0.2	0.50 ± 0.05
950	2.11 ± 0.09	0.24 ± 0.02	1.87 ± 0.09	1.20 ± 0.09	0.30 ± 0.03	0.90 ± 0.09	0.57 ± 0.05	1.2 ± 0.2	0.48 ± 0.05
1059	1.98 ± 0.09	0.28 ± 0.02	1.70 ± 0.09	1.16 ± 0.10	0.31 ± 0.02	0.85 ± 0.10	0.59 ± 0.06	1.09 ± 0.12	0.50 ± 0.06

zooplankton faecal pellets, 7 in phytoplankton, and 30 in zooplankton. Hence, $^{210}\text{Po}/^{210}\text{Pb}$ ratios higher than unity are expected to be found in fresh biogenic material, while $^{210}\text{Po}/^{210}\text{Pb}$ ratios close to unity would correspond to old material in which ^{210}Po and ^{210}Pb are in radioactive equilibrium. Our results indicate that SPM in the upper part of the water column was mainly composed of biogenic particles, whilst at greater depths, the $^{210}\text{Po}/^{210}\text{Pb}$ ratio close to unity would indicate that the material is relatively old. However, although the particulate matter collected in Niskin bottles may not be exactly the same as that which sinks to the sea floor, since along the entire water column the $^{210}\text{Po}/^{210}\text{Pb}$ ratio was slightly higher than unity (mean 1.25 ± 0.04), we conclude a contribution of biogenic material.

Imposing steady state conditions, for station A-6 a balance equation can be written as

$$F_{\text{atm}} + F_{\text{Ra}} = D + T_{\text{sink}}, \tag{5}$$

where F_{atm} is the atmospheric flux of ^{210}Pb to the sea surface, F_{Ra} is the in situ ^{210}Pb production by ^{226}Ra disintegration, D accounts for ^{210}Pb decay, and T_{sink} is the flux of ^{210}Pb due to particle sinking. Broecker and Peng (1982) estimated the atmospheric flux of ^{210}Pb (F_{atm}) for these latitudes

as $25 \text{ Bq m}^{-2} \text{ yr}^{-1}$, and more recently Rutgers van der Loeff and Berger (1991) reported a range of $2\text{--}33 \text{ Bq m}^{-2} \text{ yr}^{-1}$. From Ku and Lin (1976) and Rutgers van der Loeff and Berger (1991), an average concentration of ^{226}Ra in the water column of 3.3 Bq m^{-3} can be used, giving a ^{210}Pb flux to the sea floor in the range of $38\text{--}69 \text{ Bq m}^{-2} \text{ yr}^{-1}$. These values are less than 10% of the ^{210}Pb flux calculated from the ^{210}Pb inventory in the sedimentary column at station A-6 ($803 \pm 11 \text{ Bq m}^{-2} \text{ yr}^{-1}$). Therefore, an important net input of ^{210}Pb to the sea floor, not associated to vertical sinking of particles from the surface waters, is needed, inferring a large net advective flux of material. The findings of Palanques et al. (2002) support this conclusion, as the flux in a trap at 30 m above the bottom (mab) is about 300 times larger than that found at 500 mab. Then, it was concluded that lateral currents near the sea floor drive the transport of particles from shallow areas, causing sediment focussing in the deepest parts of the basin. This confirms the findings reported by DeMaster et al. (1991), who observed that excess ^{210}Pb inventories in the basins (mean = 45 kBq m^{-2}) were three times greater than on the shallow flanks (mean = 15 kBq m^{-2}).

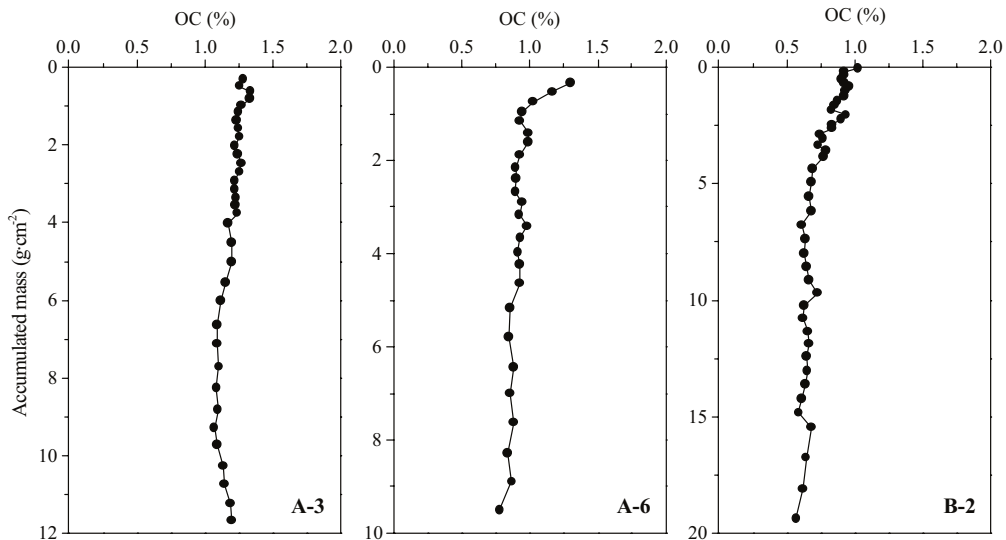


Fig. 3. Organic carbon (OC) profiles versus mass accumulation in three cores from the western Bransfield Strait.

Table 3
OC mean contents and estimates of OC burial rates and burial efficiency

Core	Mean OC contents			OC/N mean ratio	OC burial rate ^a (g C m ⁻² yr ⁻¹)	OC burial efficiency (%)
	SML (%)	Below SML (%)	All (%)			
A-3	1.25±0.04	1.12±0.04	1.20±0.07	7.1±0.3	6.7±0.4	~80
A-6	0.98±0.11	0.87±0.04	0.94±0.11	7.4±0.5	3.1±0.2	~60
B-2	0.87±0.08	0.65±0.04	0.75±0.13	7.0±0.4	6.1±0.4	~60

^a Obtained from mean OC contents below the SML and ²¹⁰Pb derived sediment accumulation rates. These values also represent the percentage of the mean annual primary production (100 g C m⁻² yr⁻¹) that accumulates to the seabed.

3.4. Organic carbon

Concentrations of organic carbon (OC) along the three sediment cores showed slight variations with depth (Fig. 3). Mean OC contents for each core were 1.20±0.07% (A-3), 0.94±0.11% (A-6) and 0.75±0.13% (B-2) if all data from the individual profiles were considered. However, and as stated before, a certain degree of mixing is present at the topmost part of the sea floor. In fact, OC contents decrease from the core surface to a constant value approximately at the lower limit of the SML. This is especially evident in core B-2 (Fig. 3). Therefore, mean values were recalculated for the SML and below it. For stations A-3 and A-6 mean concentrations are similar for both parts of the profiles taking into account associated uncertainties (Table 3), although still slightly higher in the SML. At station B-2, this difference is more pronounced. We attribute the higher contents of OC in the SML to the presence of infauna. The OC/N mean ratios in cores A-3, A-6 and B-2 were 7.1±0.3, 7.4±0.5 and 7.0±0.4, respectively (Isla, 2001), indicating that this material was close to fresh marine organic matter. As expected, no significant differences were obtained when calculating separately these mean values for the SML and below it. OC/N values also were very similar to those observed in near-bottom settling particulate matter (Palanques et al., 2002). As mid-water mean settling fluxes are negligible (0.19 mg C m⁻² d⁻¹, Palanques et al., 2002), we conclude that the organic matter accumulated in bottom sediment has the same origin as that transported laterally near the bottom. Moreover,

mean OC concentrations in particulate matter settling at 500 and 30 mab over 1 yr at station A-6 were 8.7% and 1.4%, respectively, while OC content at the surface of the sediment core A-6 was 1.3%. All these considerations agree well with the results of ²¹⁰Pb concentrations obtained in both the trapped sediment and the bottom sediment at station A-6.

Once accumulated at the surface of the bottom sediments, OC undergoes deep burial and is degraded. Maximum OC burial rates can be obtained by multiplying OC contents by sediment accumulation rates derived from ²¹⁰Pb profiles. According to the preceding remarks, we made these calculations using the OC mean values below the SML, obtaining accumulation fluxes of 6.7±0.4, 3.1±0.2 and 6.1±0.4 g C m⁻² yr⁻¹ in cores A-3, A-6 and B-2, respectively. If OC values from the SML were used, accumulation fluxes would be consequently slightly higher. These results agree with those of DeMaster et al. (1991), who reported OC contents ranging from 0.56% to 1.7% along the whole Bransfield Strait and a mean OC net flux to the bottom sediments of 7.5 g C m⁻² yr⁻¹.

Annual primary production can be estimated from the mean production over spring months, which in the study area ranges from 0.86 to 1 g C m⁻² d⁻¹ (Holm-Hansen and Mitchell, 1991; Moran and Estrada, 2002). Considering that these values are representative of the mean primary production over about 100 spring days, and assuming that the primary production is negligible during the rest of the year (Estrada, pers. comm.), we estimated that the annual primary production

in the study area is of the order of 100 g C m^{-2} . Thus, the fraction of the annual carbon accumulation flux in the sediment represents around 6–7% of the mean annual primary production in the euphotic layer for stations B-2 and A-3, and about 3% for core A-6. These values are compatible with those estimated by DeMaster et al. (1991) for the Bransfield Strait, who concluded that about 9% of the total production in surface waters (considered as $77 \text{ g C m}^{-2} \text{ yr}^{-1}$) was preserved in the seabed.

The OC burial efficiency, or the percentage of deposited OC preserved in the sediment, can be estimated by comparing the concentration at the surface of the core and the constant concentration at depth where it has undergone some diagenesis. We obtained OC burial efficiencies of about 80% at station A-3 and 60% at stations A-6 and B-2. We also can estimate burial efficiency by the following: annual OC fluxes calculated from sediment trap data at 500 and 30 mab at station A-6 (Palanques et al., 2002) were 0.35 and $18.6 \text{ g C m}^{-2} \text{ yr}^{-1}$, respectively. Taking into account that the sediment flux measured by the near bottom sediment trap was apparently almost 4 times higher than the accumulation rate derived by ^{210}Pb in bottom sediments, the annual OC accumulation rate could be near $5 \text{ g C m}^{-2} \text{ yr}^{-1}$. Therefore, both organic carbon contents and the burial rate calculated from ^{210}Pb sedimentation rates in the sea floor below the SML would be a factor 1.6 lower than the expected levels from sediment trap measurements, indicating that the OC burial efficiency would be about 60%. Remineralisation (consumption of organic matter mainly by microbial processes) occurring in the SML once OC has been deposited on the seafloor would account for remaining 40%, becoming less efficient with increasing depth in the sediment.

Acknowledgements

This research was funded by the Comisión Interministerial de Ciencia y Tecnología of Spain, under contracts ANT94-1010, MAR96-1781-CO2-01 and ANT96-1346-E. It also benefited from a pre-doctoral fellowship from CONACYT

(México), Reference 92766. We thank the officers, managers, technicians and crew of the *BIO Hespérides* and the UGBO (CSIC) for their assistance during the cruise. We also thank M. Farrán for his support during fieldwork. Comments and suggestions by O. Radakovitch and two anonymous reviewers helped to improve the manuscript.

References

- Álvarez, M., Ríos, A.F., Rosón, G., 2002. Spatio-temporal variability of air–sea carbon dioxide and oxygen fluxes in the Bransfield and Gerlache Straits during austral summer, 95–96.
- Anadón, R., Estrada, M., 2002. The FRUELA cruises. A carbon flux study in productive areas of the Antarctic Peninsula (December 1995 – February 1996). *Deep-Sea Research II* 49, 567–583.
- Anderson, J.B., Bartek, L.R., Thomas, M.A., 1991. Seismic and sedimentological record of glacial events on the Antarctic Peninsula shelf. In: Thomson, M.R.A., Crame, J.A., Thomson, J.W. (Eds.), *Evolution of Antarctica*. Cambridge University Press, Cambridge, pp. 687–691.
- Appleby, P.G., Oldfield, F., 1978. The calculation of ^{210}Pb dates assuming a constant rate of supply of unsupported ^{210}Pb to the sediment. *Catena* 5, 1–8.
- Appleby, P.G., Oldfield, F., 1992. Application of ^{210}Pb to sedimentation studies. In: Ivanovich, M., Harmon, R.S. (Eds.), *Uranium-Series Disequilibrium—Applications to Earth, Marine and Environmental Sciences*. Oxford University Press, Oxford, pp. 338–731.
- Banfield, L.A., Anderson, J.B., 1995. Seismic facies investigation of the Late Quaternary glacial history of Bransfield Basin, Antarctica. In: Cooper, A.K., Barker, P.F., Web, P.N., Brancolini, G. (Eds.), *Geology and Seismic Stratigraphy of the Antarctic Margin*. American Geophysical Union, Washington D.C, pp. 123–140.
- Bárcena, M.Á., Isla, E., Plaza, A., Flores, J.A., Sierro, F.J., Masqué, P., Sanchez-Cabeza, J.A., Palanques, A., 2002. Bioaccumulation record and paleoclimatic significance in the Western Bransfield Strait. The last 2000 years. *Deep-Sea Research II* 49, 935–950.
- Benninger, L.K., Aller, R.C., Cochran, J.K., Turekian, K.K., 1979. Effects of biological mixing on the ^{210}Pb chronology and trace metal distribution in a Long Island Sound sediment core. *Earth and Planetary Science Letters* 43, 241–259.
- Broecker, W.S., Peng, T.-H., 1982. *Tracers in the Sea*. Lamont-Doherty Geological Observatory. Columbia University, NY.
- Canals, M., Urgeles, R., Calafat, A.M., 2000. Deep-sea floor evidence of past ice streams off the Antarctic Peninsula. *Geology* 28 (1), 31–34.

- Cochran, J.K., 1985. Particle mixing rates in sediments of the eastern equatorial Pacific. Evidence from ^{210}Pb , $^{239,240}\text{Pu}$ and ^{137}Cs distributions at MANOP sites. *Geochimica et Cosmochimica Acta* 45, 1155–1172.
- DeMaster, D.J., Cochran, J.K., 1982. Particle mixing rates in deep-sea sediments determined from excess ^{210}Pb and ^{32}Si profiles. *Earth and Planetary Science Letters* 61, 257–271.
- DeMaster, D.J., Nelson, T.M., Harden, S.L., Nittrouer, C.A., 1991. The cycling and accumulation of biogenic silica and organic carbon in Antarctic deep-sea and continental margin environments. *Marine Chemistry* 35, 489–502.
- DeMaster, D.J., Ragueneau, O., Nittrouer, C.A., 1996. Preservation efficiencies and accumulation rates for biogenic silica and organic C, N, and P in high-latitude sediments: The Ross Sea. *Journal of Geophysical Research* 101 (C8), 18051–18518.
- Goldberg, E.D. 1963. Geochronology with ^{210}Pb in radioactive dating. IAEA, Vienna, 121–131.
- Goldberg, E.D., Koide, M., 1962. Geochronological studies of deep-sea sediments by the ionium-thorium method. *Geochimica et Cosmochimica Acta* 26, 417–450.
- Gràcia, E., Canals, M., Farràn, M., Sorribas, J., Pallàs, R., 1997. Central and Eastern Bransfield Basins (Antarctica) from high resolution swath-bathymetry data. *Antarctic Science* 9, 168–180.
- Guinasso, N.L., Shink, D.R., 1975. Quantitative estimates of biological mixing rates in abyssal sediments. *Journal of Geophysical Research* 80 (21), 3032–3043.
- Harden, S.L., DeMaster, D.J., Nittrouer, C.A., 1992. Developing sediment geochronologies for high-latitude continental shelf deposits: a radiochemical approach. *Marine Geology* 103, 69–97.
- Heinze, C., Jansen, E., Ragueneau, O., van den Berg, C.M.G., Watson, A.K., 1999. Global carbon balance. In: Oost, W., and Lipiatou, E. (Eds.), *Air–sea and sea–ice interactions*. Research in enclosed seas series-7. EUR 18638 EN, pp 36.
- Heussner, S., Cherry, R.D., Heyraud, M., 1990. ^{210}Po , ^{210}Pb in sediment trap particles on a Mediterranean continental margin. *Continental Shelf Research* 10, 989–1004.
- Heyraud, M., Cherry, R.D., 1983. Correlation of ^{210}Po and ^{210}Pb enrichments in the sea-surface microlayer with neuston biomass. *Continental Shelf Research* 1, 283–293.
- Holm-Hansen, O., Mitchell, B.G., 1991. Spatial and temporal distribution of phytoplankton and primary production in the Western Bransfield Strait region. *Deep-Sea Research* 38 (8/9), 961–980.
- Holler, P., 1989. Mass physical properties of sediments from Bransfield Strait and Northern Weddell Sea. *Marine Geotechnology* 8, 1–18.
- Huntley, M., Karl, D.M., Niler, P., Holm-Hansen, O., 1991. Research on Antarctic ecosystem rates (RACER): an interdisciplinary field experiment. *Deep-Sea Research* 38 (8/9), 911–941.
- Isla, E., 2001. Downward particle fluxes and sediment accumulation rates related to the organic carbon and biogenic silica cycles in the Gerlache and Western Bransfield Straits, Antarctica. Ph.D. Thesis, Universitat Politècnica de Barcelona, 250 pp., unpublished.
- Keeling, C.D., Whorf, T.P., 1999. Atmospheric CO_2 records from sites in the SIO air sampling network. In: *Trends: A Compendium of Data on Global Change*. Carbon Dioxide Information Analysis Center, Oak Ridge National Laboratory, US Department of Energy, Oak Ridge, TN, USA.
- Koide, M., Soutar, A., Goldberg, E.D., 1972. Marine geochemistry with ^{210}Pb . *Earth and Planetary Science Letters* 14, 442–446.
- Koskelo, M.J., Aarnio, P.A., Routti, J.T., 1981. SAMPO80: minicomputer program for gamma spectrum analysis with nuclide identification. *Computer Physics Communications* 24, 11–35.
- Ku, T.-L., Lin, M.-C., 1976. ^{226}Ra distribution in the Antarctic Ocean. *Earth and Planetary Science Letters* 32, 236–248.
- Ledford-Hoffman, P.A., DeMaster, D.J., Nittrouer, C.A., 1986. Biogenic-silica accumulation in the Ross Sea and the importance of Antarctic continental-shelf deposits in the marine silica budget. *Geochimica et Cosmochimica Acta* 50, 2099–2110.
- Marland, G., Boden, T.A., Andres, R.J., Brenkert, A.L., Johnston, C. 1999. Global, Regional, and National CO_2 Emissions. In: *Trends: A Compendium of Data on Global Change*. Carbon Dioxide Information Analysis Center, Oak Ridge National Laboratory, US Department of Energy, Oak Ridge, TN, USA.
- Moran, X.A.G., Estrada, M., 2002. Phytoplanktonic DOC and POC production in the Bransfield and Gerlache Straits as derived from kinetic experiments of ^{14}C incorporation. *Deep-Sea Research* II 49, 769–786.
- Neftel, A., Moor, E., Oeschger, H., Stauffer, B., 1985. Evidence from polar ice cores for the increase in atmospheric $p\text{CO}_2$ in the past two centuries. *Nature* 315, 45–47.
- Nelson, T.M., 1988. Biogenic silica and carbon accumulation in the Bransfield Strait, Antarctica, MS Thesis, North Carolina State University, Raleigh NC, 89 pp.
- Nittrouer, C.A., DeMaster, D.J., McKee, B.A., Cuthall, N.H., Larsen, L.I., 1984. The effect of sediment mixing on ^{210}Pb accumulation rates for the Washington continental shelf. *Marine Geology* 31, 297–316.
- Nozaki, Y., Cochran, J.K., Turekian, K.K., Keller, G., 1977. Radiocarbon and ^{210}Pb distribution in submersible-taken deep-sea cores from project FAMOUS. *Earth and Planetary Science Letters* 34, 167–173.
- Palanques, A., Isla, E., Puig, P., Sanchez-Cabeza, J.A., Masqué, P., 2002. Annual evolution of downward particle flux during the FRUELA project Western Bransfield Strait in the (Antarctica). *Deep-Sea Research* II 49, 903–920.
- Roberts, K.A., Cochran, J.K., Barnes, C., 1997. ^{210}Pb and $^{210,240}\text{Pu}$ in the Northeast Water Polynya, Greenland: particle dynamics and sediment mixing rates. *Journal of Marine Systems* 10, 401–413.
- Rutgers van der Loeff, M.M., Berger, G.W., 1991. Scavenging and particle flux: seasonal and regional variations in the

- Southern Ocean (Atlantic sector). *Marine Chemistry* 35, 553–567.
- Sanchez-Cabeza, J.A., Masqué, P., Ani-Ragolta, I., 1998. Pb-210 and Po-210 analysis in sediments and soils by microwave acid digestion. *Journal of Radioanalytical and Nuclear Chemistry* 227, 19–22.
- Sanchez-Cabeza, J.A., Masqué, P., Ani-Ragolta, I., Merino, J., Frignani, M., Alvisi, F., Palanques, A., Puig, P., 1999. Sediment accumulation rates in the Southern Barcelona continental margin (NW Mediterranean Sea) derived from ^{210}Pb and ^{137}Cs chronology. *Progress in Oceanography* 44 (1-3), 313–332.
- Sanchez-Cabeza, J.A., Ani-Ragolta, I., Masqué, P., 2000. Some considerations of the ^{210}Pb constant rate of supply (CRS) dating model. *Limnology and Oceanography* 45 (4), 990–995.
- Sarmiento, J.L., Toggweiler, J.R., 1984. A new model for the role of the oceans in determining $p\text{CO}_2$. *Nature* 308, 621–624.
- Thunell, R.C., Moore, W.S., 1994. Elemental and isotopic fluxes in the Southern California Bight: a time-series sediment trap study in the San Pedro Basin. *Journal of Geophysical Research* 99, 875–889.
- Tsunogai, S., Kurata, T., Suzuki, T., Yokota, K., 1988. Seasonal variation of atmospheric ^{210}Pb and Al in the Western North Pacific Region. *Journal of Atmospheric Chemistry* 7, 389–407.
- Turekian, K.K., Nozaki, Y., Benninger, L.K., 1977. Geochemistry of atmospheric radon and radon products. *Annual Review of Earth and Planetary Science Letters* 5, 227–255.
- Walsh, J.J., Premuzic, E.T., Gaffney, J.S., Rose, G.T., Harbottle, T., Stoenner, R.W., Balsam, W.L., Betzer, P.R., Macko, S.A., 1985. Organic storage of CO_2 on the continental slope off the mid-Atlantic Bight, the South-eastern Bering Sea and the Peru Coast. *Deep-Sea Research* 32, 853–883.
- Yoon, H.I., Han, M.W., Park, B.K., Oh, J.K., Chang, S.K., 1994. Depositional environment of near-surface sediments, King George Basin, Bransfield Strait, Antarctica. *Geomarine Letters* 14, 1–9.
- Zuo, Z., Eisma, D., Gieles, R., Beks, J., 1997. Accumulation rates and sediment deposition in the Northwestern Mediterranean. *Deep-Sea Research Part II* 44 (3-4), 597–609.